

Simulation analysis of the EUSAMA Plus suspension testing method including the impact of the vehicle untested side

K Dobaj¹

¹ Institute of Automobiles and Internal Combustion Engines, Cracow University of Technology, Al. Jana Pawla II 37, 31-864 Krakow, Poland;

E-mail: kdobaj@pk.edu.pl

Abstract. The work deals with the simulation analysis of the half car vehicle model parameters on the suspension testing results. The Matlab simulation software was used. The considered model parameters are involved with the shock absorber damping coefficient, the tire radial stiffness, the car width and the rocker arm length. The consistent vibrations of both test plates were considered. Both wheels of the car were subjected to identical vibration, with frequency changed similar to the EUSAMA Plus principle. The shock absorber damping coefficient (for several values of the car width and rocker arm length) was changed on one and both sides of the vehicle. The obtained results are essential for the new suspension testing algorithm (basing on the EUSAMA Plus principle), which will be the aim of the further author's work.

1. Introduction

Increasing number of vehicles in use requires continuous improvement of the car diagnostics methods, especially related to active safety. The car suspension is one of the most important assemblies in relation not only with active safety but also with ride comfort. The suspension diagnostic methods must follow the specified requirements. The diagnosis must be relatively fast and easy to perform. Furthermore, differences in the car suspension design must not influence on the formulated suspension condition indicators. Indicators must give clear values for one state of the car suspension damage. These requirements must be able to application in the test stand which corresponds to in-road driving as far as it is possible.

Suspension quality, referring to active safety and ride comfort, results in the vehicle behaviour under the influence of the road unevenness. The test stand methods analyse the vehicle response under the provoked regular vibrations. Several testing methods are developed [1,2,3]. These methods vary in the amplitude of the excitation. The exciter (steel plate on which the car wheel is placed) is supplied with constant frequency with value over the two vehicle resonance frequencies (from sprung and unsprung mass). The excitation frequency is maintained for few seconds and then the idle run takes place. The behaviour of the test stand- vehicle assembly during the phase of damping is analysed. For the determination of the suspension, several testing indicators were formulated. Some of them are related with the value of the exciter amplitude while passing through the resonance frequencies [2,3], some refer to the damping ratio calculation (in ex. according to Lehr) [3]. Another indicators are related with the force of the load exerted on the exciter plate from the wheel and mass of the quarter of the vehicle.



The suspension test stands vary in the construction but all of them consider only one wheel of the vehicle and its loading mass during single testing cycle. Thus, the effects of interaction between two sides of the vehicle are neglected. These effects include car transverse moves and influence of

damping qualities of the side of the vehicle, on which the suspension criteria are not calculated. The author conducted simulation analysis the modification of the EUSAMA Plus suspension testing method. The modification introduced consistent vibrations of both sides of the vehicle.

2. Suspension testing methods development

The issues of determination of the vehicle parameters influence on active safety and comfort criteria indicated on the test stands were considered by many authors. Innovative conceptions of the EUSAMA Plus suspension testing method were introduced in work [1]. The author of that paper formulated automatic diagnostic method based on the neural network system. The neural network was used to conduct the image analysis involved with the EUSAMA rate (WE). The analysed images were formulated as a figures of the EUSAMA rate change during the time of the measurement. The measurement was performed according to the EUSAMA plus testing principle. The excitation frequency was changed from 30 Hz to 1 Hz. Each value of the frequency, with step of 1 Hz, was maintained in 5 seconds. Damping qualities of the passive shock absorber were analysed. Simulation model was formulated [1]. The model included characteristics of the shock absorber with the level of hydraulic fluid varied from 100 % to 25 % with the step of 25 %. The characteristics of shock absorbers with different levels of hydraulic fluid included in the simulation model were obtained experimentally [1]. Different levels of the hydraulic fluid resulted in different values of the EUSAMA rate and provoked shift of the range of maximal EUSAMA rate (minimum of the test plate loading force). Formulated automatic classifier (based on neural network system) analysed the figures and immediately matched considered state of damage in shock absorber (loss of hydraulic fluid) into one of four states of the suspension (mostly shock absorber) condition. The results proved that the neural network application is an appropriate way of EUSAMA suspension testing improvement.

Another approach of the suspension testing method development is involved with the vibroacoustics vibrations analysis [2]. The analysis is focused on determination of the kind of the shock absorber damage. Measurements were conducted on the EUSAMA test stand, but additional transmitters were mounted on the vehicle body and the rocker arm. It allowed for the measurement of the relative acceleration between the sprung and unsprung mass (joined by, among other, shock absorber). The measured acceleration values underwent the discretization process. After this process the signals were processed by following two-dimensional methods: Fast Fourier Transformation, Wavelet Transform, Wigner- Ville Distribution [2]. The processed signals analysis was oriented on application of the signal processing methods application to determination of the kind of the shock absorber failure. The time- frequency spectra of the relative shock absorber accelerations were created. The created spectra were involved with standard shock absorber and shock absorber with 25 % hydraulic fluid volume loss. Relatively small volume losses (25 %) provoke increases of the acceleration in the range of excitation frequencies over the resonance. Furthermore vibroacoustics method of the shock absorbers diagnostics was proposed [2]. The method was based on the wavelet transform, which allows the adjustment of the observation range and analysis of the time- frequency characteristics in the short, selected range. The new diagnostic estimator was created. The estimator allowed for detection of the kind of the shock absorber failure.

In the work [3], the comparison of suspension (referenced mostly to shock absorber) diagnostic methods was conducted. The authors described following methods: BOGE, EUSAMA, modified BOGE method, phase shift principle and Theta principle. The experimental analysis was performed. The modified BOGE method was introduced by MAHA company. The car wheel is placed on the testing plate joined with crank mechanism of the exciter and also supported on the ground by the coil spring [3].

The measurement system allowed for measurement of exciter plate amplitude and also the force exerted on the plate during the testing cycle. The suspension efficiency percentage indicator is calculated according to the algorithm specified by MAHA company. The phase shift method consists in determining the phase angle between the signals amplitude and force acting on the exciter plate.

The suspension criterion is defined as the minimal value of the angle in the range of frequency between the resonance of the sprung and unsprung mass. Development of the suspension testing is now strongly concerned with Theta principle. The principle uses the test stand similar to BOGE method. The footprint plate is excited to the frequency of 10 Hz. Then the propulsion is disconnected and the idle run occurs [3]. On the basis of the measured parameters, the damping ratio according to Lehr is calculated. It is defined as a ratio of linear suspension damping to the critical value of damping. The definition is correct for the mechanical assembly with 1 DOF. The quarter of car- test stand assembly has 3 DOF. Thus the manufacturers apply simplifying algorithms in the Lehr damping ratio calculations. The optimal Lehr damping ratio for the car with new shock absorber is determined in the range from 0.25 to 0.35. In the work [3] the experimental analysis was conducted. The analysis was involved with verification of the influence of the unsprung mass and tyre pressure change on results of the suspension testing according to EUSAMA and Theta testing principles. The Theta principle is much less sensitive to the considered parameters change in comparison with the EUSAMA principle. The shock absorber parameters, obtained during the tester plate excitation can be also used for the vehicle suspension modelling [6]. The tested suspension parameters are measured while the test stand excitation run performed is. The accelerometers, strain gauges and race transducers, mounted on the shock absorber, are used. The another approach of the additional sensors usage is introduced in the work [7] and [9]. The sensors which are attached to the shock absorbers are used. The micro-mechanical sensors measure the acceleration and the internal pressure of the shock absorber [9]. Furthermore, the oil temperature measured is [7,9]. The continuous monitoring, during complete driving cycles, allows for the shock absorber replacement before its damping qualities decrease rapidly. For the shock absorbers diagnosis, the artificial intelligence was also adapted. The work [8] describes the application of the neural network with its training and testing process.

3. Simulation analysis

3.1. The model formulation

To conduct the vibrational analysis, a numerical model was formulated. The Matlab simulation software was used. The half- car vehicle model was developed as the assembly of two quarter- car vehicle models. The sprung masses were modelled as concentrated points, joined by the massless lever (the half of the lever with the length x). The lever was joined to another lever which corresponded to the anti- roll bar of the car (length of the half of the anti- roll bar described by y). The sprung masses were joined to the rocker arms with dimensions a and b (Fig.1) via shock absorber and coil spring with the replacement damping and stiffness. To the endings of the rocker arms the unsprung masses were joined. The unsprung masses were supported on the test stand plates with masses m_p . The plates are coupled with the crank mechanisms, with radiuses r , joined to the frequency sources.

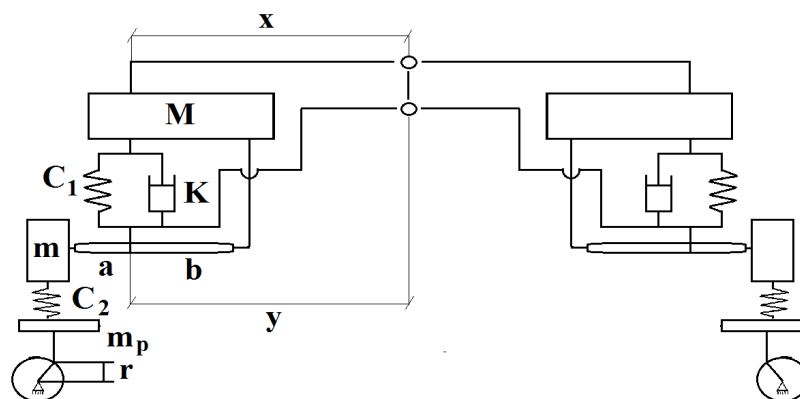


Figure 1. The scheme of the simulation model.

Table 1. The simulation model parameters

Mass parameters			Stiffness parameters:		
M	270	kg	C₁	45000	N/m
m	40	kg			
m_p	15	kg	C₂	200000	N/m

Shock absorber damping K			Dimensional parameters		
K	1748	Ns/m	x	0.844	m
a	0.1	m	y	0.744	m
b	0.4	m	r	3	mm

The car wheel suspension was simplified as an assembly of the rocker arm, perpendicularly joined to the spring and the damper. Thus, the inclination of the suspension column was neglected. Further simplifying assumptions were involved with the replacement parameters. The nonlinear passive shock absorber was modelled as a linear damper with the replacement damping coefficient K . The base value of the damping coefficient was calculated correspondingly to the car mass parameters, in the formula described in [4]. The suspension spring element (a coil spring) was described by replacement stiffness coefficient C_1 . The tyre was modelled by one parameter- the radial stiffness C_2 . The model parameters are included in Tab.1 The mass and dimensional parameters refer to the Fiat Grande Punto, with the parameters obtained in [5].

3.3. Results of the analysis

The simulation was conducted basing on the half car vehicle model, subjected to uniform vibrations of the tester plates. The frequency applied to the test stand crank mechanisms was changed from 1 to 30 Hz with the step of 1 Hz per second (similar to the EUSAMA Plus testing principle). During every simulation attempt, the tester plate dynamic force was measured. The measurement was conducted on the one side of the test stand- vehicle assembly. The maximum of this force occurred in different frequency ranges according to considered simulation scenario. The simulation scenarios were involved with applying the same frequency, changed in the same time periods, to both tester plates. This approach was conducted as a step for the EUSAMA Plus method modification. The modification takes into account the influence of the suspension condition of the vehicle untested side. The knowledge of the system properties in terms of the vibrations transmission from the one to another

side of the vehicle will be essential for the new testing algorithm formulation (as a modification of the EUSAMA Plus method). The algorithm will be the object of the author’s further work.

3.3.1 Influence of shock absorber damping coefficient

The first simulation scenario was involved with the change of the shock absorber damping coefficient. The analysis results are included in Tab. 2. Each value of the damping coefficient was changed on the only one vehicle side (where the plate dynamic force was measured) and on both sides. The EUSAMA coefficient values for the parameter change on one and both sides are labelled “EUS., tested” and “EUS., both” respectively (Tab. 2). Furthermore the ranges of frequency, where the maximal dynamic force occurred are also included in the way that “f. range” label is placed above and under the corresponding “EUS., tested” and “EUS., both” table field.

Table 2. Influence of the shock absorber damping coefficient on the EUSAMA coeff.

damp. coeff.	1748 [Ns/m]	1448 [Ns/m]	1148 [Ns/m]	848 [Ns/m]	548 [Ns/m]	448 [Ns/m]
f. range	15-25 Hz	15-25 Hz	15-25 Hz	15-25 Hz	15-25 Hz	15-25 Hz
EUS., tested	0.69	0.68	0.66	0.65	0.62	0.61
EUS., both	0.69	0.66	0.62	0.55	0.33	0.22
f. range	15-25 Hz	15-25 Hz	15-25 Hz	5-15 Hz	5-15 Hz	5-15 Hz
damp. coeff.	348 [Ns/m]	148 [Ns/m]	98 [Ns/m]	48 [Ns/m]	18 [Ns/m]	8 [Ns/m]
f. range	15-25 Hz	15-25 Hz	15-25 Hz	5-15 Hz	5-15 Hz	5-15 Hz
EUS., tested	0.61	0.59	0.58	0.57	0.56	0.56
EUS., both	0.03	0	0	0	0	0
f. range	5-15 Hz	5-15 Hz	5-15 Hz	5-15 Hz	5-15 Hz	5-15 Hz

The obtained results confirmed the commonly known disadvantage of the suspension diagnostics methods. The methods react only to prominent decreases of the shock absorber damping force. The conditions of the simultaneous excitation of the plates with the same frequency provoked the behaviour of the parallel coupling of the shock absorber. In the case of the damping coefficient decrease only in the “tested” model side, the EUSAMA coefficient maintained its value corresponding to the very good damping conditions (exceeding 0,6) in the range of damping coefficient from 1748 to 348 Ns/m. From 148 to 8 Ns/m the EUSAMA coefficient value referred to good damping condition range (from 0,6 to 0,4). The damping coefficient 1748 Ns/m maintained on the untested side of the model supported the poor damping qualities of the tested side and provoked limited decrease of the EUSAMA coefficient.

In the case of the damping coefficient change on both sides, the model response is more significant. The damping coefficient deterioration from 1748 to 548 Ns/m provides the change of the EUSAMA Coefficient from 0.69 to 0.33. This change corresponds to descriptively suspension damping change from very good (0,69) to satisfactory (0,33). The model reaction is involved with the uniform damping qualities deterioration of both shock absorbers, mounted in parallel. The change damping coefficient from 348 to 8 Ns/m results in the complete lack of the vibrations damping, resulting in the achievement of the 0 EUSAMA coefficient. This value refers to the detachment between the tire and the tester plate.

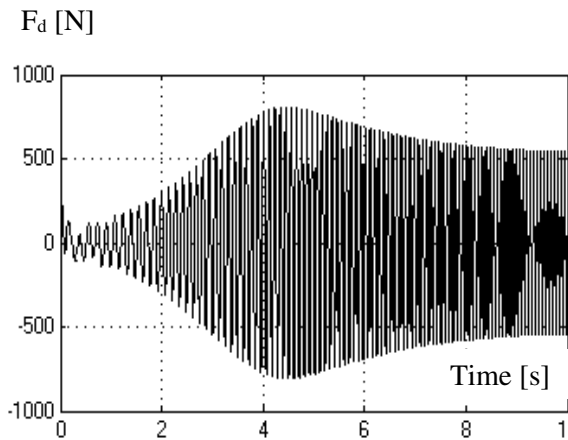


Figure 2. Time change of the force F_d , 1448 Ns/m on both sides, f. range 5-15 Hz.

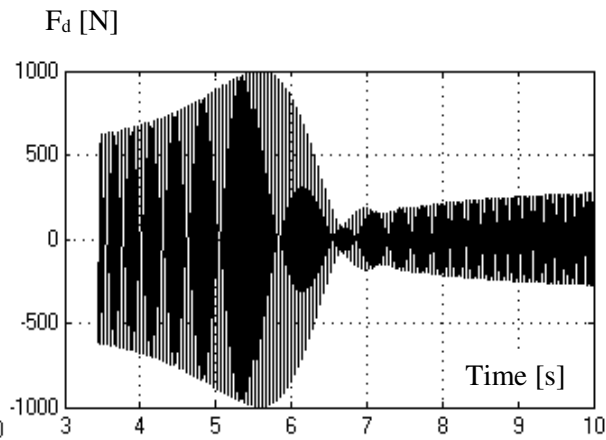


Figure 3. Time change of the force F_d , 1448 Ns/m on one side, f. range 15-25 Hz.

The time change of the plate dynamic force (F_d) in the selected simulation cases is shown in every figure of the article. The Fig. 2 and 3 show the testing process in the range from 5 to 25 Hz, with the frequency change speed 1_Hz per second. The process took 20 seconds and was divided in the two simulation scenarios. During the frequency change, the resonances of sprung and unsprung mass occur. The smaller frequency value, obtained about 4 second (Fig. 2) corresponds to the resonance of the sprung mass. Whereas, the frequency value obtained about 5,5 second in the process of frequency change from 15 to 25 Hz (Fig.3) corresponds to the resonance of the sprung mass. The maximal dynamic force value is obtained in the resonance frequencies. It is noticeable that decrease of the global damping coefficient of the half car model assembly provides that the frequency range of the maximal damping force occurrence is postponed from bigger to lower values. Due to the decreased global damping, the assembly vibrations are increased. In these conditions, the inertia of a large sprung mass vibrating with a large resonance amplitude is responsible for the maximal dynamic force value. This phenomenon is shown in Fig 4 and 5, where the low damping conditions are presented. In the situation in Fig.5, the plate dynamic force is about 7000 N, which exceeds the wheel static load force for more than 50 %.

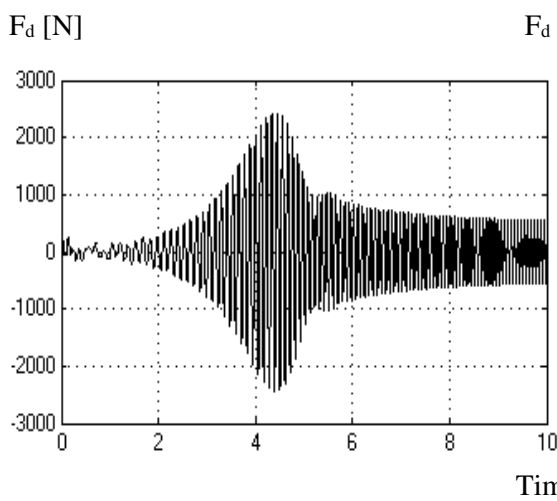


Figure 4. Time change of the force F_d , 448 Ns/m on both sides, f. range 5-15 Hz.

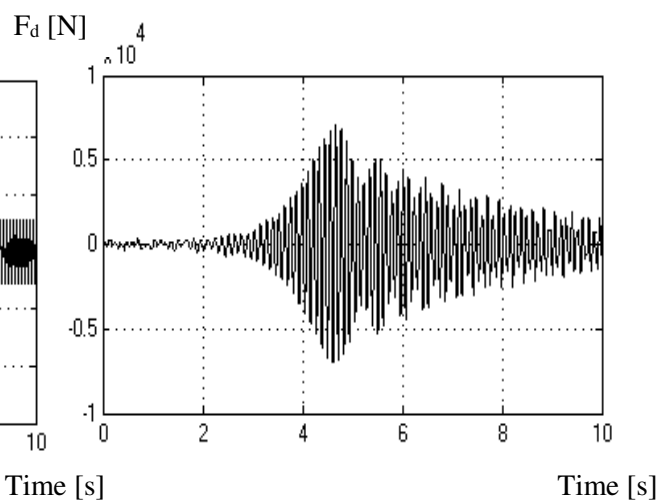


Figure 5 Time change of the force F_d , 48 Ns/m on both sides, f. range 15-25 Hz.

3.4.2 Influence of tire radial stiffness

Another simulation scenario was involved with the tire radial stiffness change. The change range of the considered parameter was selected to analyse the influence of different tire pressure and application of the tires, varied in their profiles.

Table 3. The analysis of the tire radial stiffness influence

radial stiff.	50000 [N/m]	100000 [N/m]	150000 [N/m]	200000 [N/m]	250000 [N/m]	300000 [N/m]
f. range	15-25 Hz	15-25Hz	15-25 Hz	15-25 Hz	15-25 Hz	15-25 Hz
EUS., tested	0.85	0.8	0.74	0.69	0.64	0.59
EUS., both	0.77	0.74	0.78	0.69	0.66	0.65
f. range	15-25 Hz	5-15 Hz	5-15 Hz	15-25 Hz	15-25 Hz	20-30 Hz

Results of the tire radial stiffness influence are included in Tab. 3. The table fields “EUS., tested” and “EUS., both” contain the EUSAMA coefficient values obtained in the previously described manner. The “f. range” captions above and under the EUSAMA coefficient values refer to the “EUS., tested” and “EUS., both” table field respectively. The increase of the tire radial stiffness provokes the deterioration of the EUSAMA coefficient value (Tab. 3). However the parameter change in the considered range, allows for maintaining the EUSAMA coefficient in the range corresponding to very good damping conditions. The value 50000 N/m of the radial stiffness allows for the achievement of very beneficial (according to ride comfort) value of the EUSAMA coefficient, but such low radial stiffness may provoke the loss of the vehicle stability. The Fig 6 shows the change of the dynamic force of the tester plate in the considered conditions. In addition to low value of its maximum, the regularity (small changes) of the force is noticeable. The regularities result in high comfort, perceptible by the car passengers. On the other hand, when the tyre radial stiffness is high (Fig. 7), the tester plate dynamic force shows rapid decrease in the considered frequency range. The stiffer tyre undergo smaller displacements in the specified excitation conditions, which results in higher test plate dynamic forces. The decrease influences both active safety and ride comfort of the vehicle. The road vibrations (resulting in the force changes) may cause that the car reaction, provoked by the driver’s steering is different than expected. The influence of the one side of the vehicle to another is also noticed. When the global value (as a parallel springs assembly) of tyre radial stiffness coefficient is lower, the EUSAMA coefficient takes more beneficial values (Tab. 3).

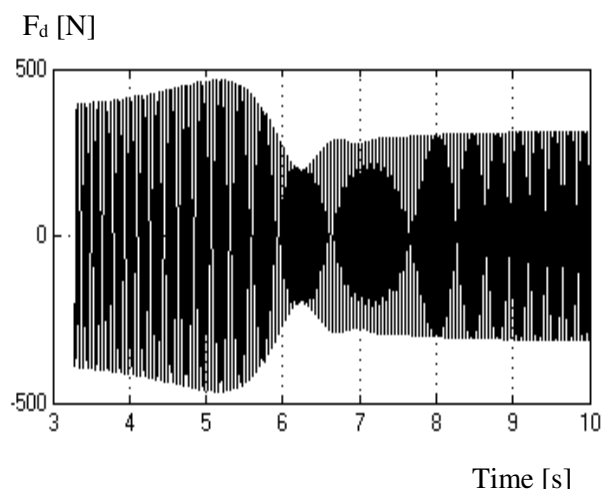


Figure 6. Time change of the force F_d , 50000 N/m on one side, f. range 15–25 Hz.

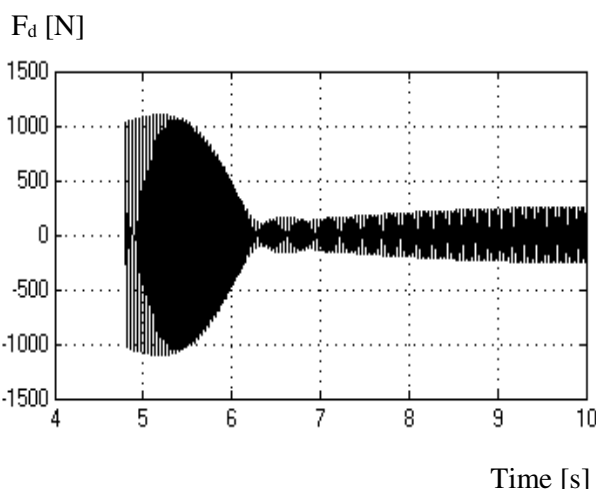


Figure 7. Time change of the force F_d , 300000 N/m on both sides, f. range 5-25 Hz.

3.4.3 Influence of the car width

To analyse the testing method sensitivity on the parameters of various vehicles, the influence of the car width was examined. Three width values were considered (Tab. 4). The simulation attempts were performed in the conditions of high (1748 Ns/m), medium (1000 Ns/m) and low (20 Ns/m) shock absorber damping coefficients, changed on the “tested” and both model sides.

Table 4. The results of the car width influence analysis.

Car width / frequency range	EUS., tested/ both 1748 [Ns/m]	EUS., tested 1000 [Ns/m]	EUS., both 1000 [Ns/m]	EUS., tested 20 [Ns/m]	EUS., both 20 [Ns/m]
fr. range 1,588 m	15-25 Hz 0.69	15-25 Hz 0,66	15-25 Hz 0.6	5-15 Hz 0.56	5-15 Hz 0
fr. range 1,688 m	15-25 Hz 0.69	15-25 Hz 0.65	15-25 Hz 0.6	15-25 Hz 0.57	5-15 Hz 0
fr. range 1,788 m	15-25 Hz 0,69	15-25 Hz 0.65	15-25 Hz 0.6	5-15 Hz 0.56	5-15 Hz 0

The model response proved very small sensitivity on the car width change. As in the previous simulation scenarios the poor damping condition of one side of the vehicle provide that the influence of vibrations meets the resistance from the other side of the vehicle, considering the leverage between the suspension elements. The increased vehicle width must provide that the influence of the damping of one side to another decreased is. However, in the considered width range, this decrease is negligibly small (Tab.4). The conditions of medium damping coefficient values are shown in Fig. 8. Whereas, the conditions of poor damping are shown in Fig. 9. The indicated in these figures changes of the test plate dynamic force are similar to the previously obtained results, in similar model damping qualities.

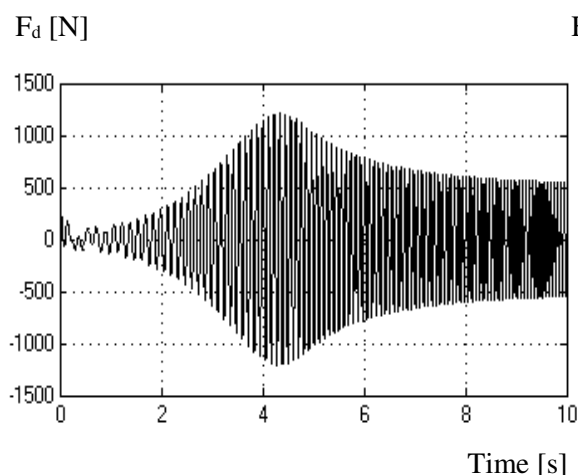


Figure 8. Change of the force F_d , 1000 Ns/m on both sides, width 1,588 m, f. 15–25 Hz.

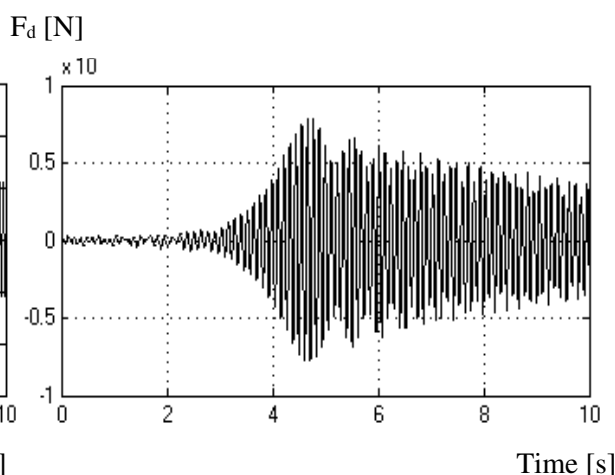


Figure 9. Change of the force F_d , 20 Ns/m on both sides, width 1,788 m f. 5-25 Hz.

3.4.3 Influence of the rocker arm length

Another simulation scenario referred to the suspension leverage change. It was modelled by adjusting the rocker arm length. The distance between the rocker support and the point of the suspension-

damping column was changed (distance “b”, look at chapter 3.1). The situations referred to the high, medium and poor damping conditions, for the tested and both sides of the vehicle.

Table 5. The rocker arm length change influence on the EUSAMA coeff.

distance b / frequency range	EUSAMA tested/ untested 1748 [Ns/m]	EUS., tested 1000 [Ns/m]	EUS., both 1000 [Ns/m]	EUS., tested 20 [Ns/m]	EUS., both 20 [Ns/m]
fr. range	15-25 Hz	15-25 Hz	5- 15 Hz	5- 15 Hz	5- 15 Hz
30 cm	0.67	0.62	0.56	0.51	0
fr. range	15-25 Hz	15-25 Hz	15-25 Hz	15-25 Hz	5-15 Hz
40 cm	0.69	0.65	0.6	0.57	0
fr. range	15-25 Hz	15-25 Hz	15-25 Hz	15-25 Hz	5- 15 Hz
50 cm	0.7	0.67	0.61	0.59	0

The rocker arm length has small impact on the EUSAMA coefficient value (Tab.5), but the influence is more significant than the car width changes. The increased distance between the rocker arm support and the suspension- damping column mounting position results in the increase of the EUSAMA coefficient value. This phenomenon can be explained by the decreased relative displacement of the parts of the shock absorber, under the specified excitation conditions, when the considered distance is extended. Decrease of the relative displacement provokes the smaller values of the tester plate dynamic force. The comparison of the dynamic force change under the same excitation conditions, exerted on the two suspension assemblies, varied in the rocker lengths, is shown in Fig. 10 and 11. The figures refer to the simulation scenarios marked in white font in the Tab. 6. The increase of the length from 30 (Fig. 10) to 50 cm (Fig. 11) in the considered conditions, results in the improvement of the EUSAMA coefficient from 0.62 to 0.67 (Tab. 6).

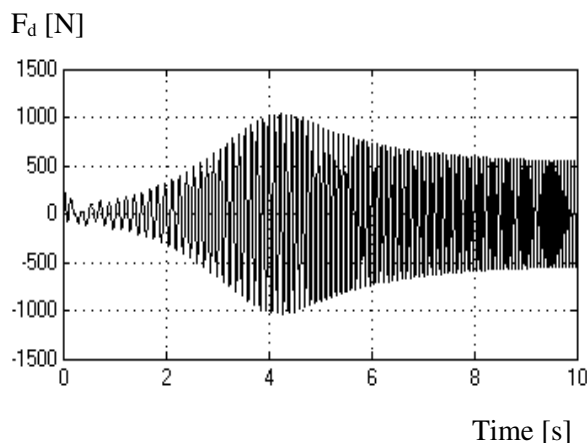


Figure 10. Time change of the force F_d , 1000 Ns/m on one side, $b= 30$ cm f. range 15–25 Hz.

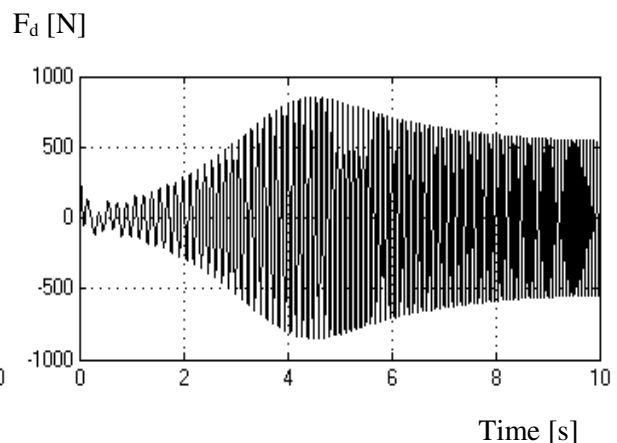


Figure 11. Change of the force F_d , 1000 Ns/ m on one side, $b= 50$ cm f. range 5-25 Hz.

4. Conclusions

The first simulation scenario considered the influence of the shock absorber damping coefficient. Change of the considered parameter in only one side of the vehicle provokes that the damping qualities of the non-changed side strongly affect the changed side. The second simulation scenario referred to the tire radial stiffness change. Increase of the parameter results in the deterioration of the EUSAMA coefficient values. The third scenario was involved with the analysis of the car width influence. The extended width (from 1.588 m to 1.788 cm) provided that the influence of the one side damping qualities to another was deteriorated but the changes were very small. The last scenario referred to the rocker arm length changes. The increase of the length provokes smaller relative displacements of the suspension- damping column and provides increased EUSAMA coefficient values. The influence (in the considered range from 30 to 50 cm) provides small changes. But they are more significant from the case of the car width changes. The conducted analysis corresponds to the conditions of passing through the perpendicular, symmetrical road unevenness, acting simultaneously on the both sides of the car. Real example of these conditions is involved with passing through the speed bump. The obtained results constitute the step for the formulation of the new suspension testing algorithm (as a modification of the EUSAMA Plus principle), which will be the object of the Author's further work.

References

- [1] Cempiel D 2013 *Automatic Classifier of the Kind of Car Shock Absorber Damage* Combustion Engines 154(3) pp 1067-1075
- [2] Gardulski J 2006 *Badania Diagnostyczne Amortyzatorów* DIAGNOSTYKA'2 (38) pp 187-198
- [3] Stańczyk T L and Jurecki R 2014 *Analiza Porównawcza Metod Badania Amortyzatorów Hydraulicznych* ZESZYTY NAUKOWE INSTYTUTU POJAZDÓW 4(100) pp 25-45
- [4] Mitschke M. and Wallentowitz H 2004 *Dynamik der Kraftfahrzeuge, 4. Auflage*, Springer Verlag, Berlin/Heidelberg
- [5] Ślaski G and Grześkowiak P 2011 *Masy Nieresorowane- Analiza Mas Elementów Konstrukcyjnych Zawiesznień Samochodów Osobowych* Logistyka 6/2011 pp 3743- 3750
- [6] Popescu M O S and Mastorkakis N E 2009 *Testing and Simulation of a Motor Vehicle Suspension* INTERNATIONAL JOURNAL OF SYSTEMS APPLICATIONS, ENGINEERING & DEVELOPMENT Issue 2, 3/2009 pp 74- 83
- [7] Ferreira C Ventura P Grinde C Morais R Valente A Neves C and Reis M 2010 *Characterization and testing of a shock absorber embedded sensor* Procedia Engineering 5/2010 pp 319- 322
- [8] Sincebaugh P Green W and Rinkus G 1996 *A neural network based diagnostic test system for armored vehicle shock absorbers* Expert System with Applications vol. 11 issue 2 pp 237- 244
- [9] Ferreira C Ventura P Grinde C Morais R Valente A Neves C and Reis M 2009 *A novel monolithic silicon sensor for measuring acceleration, pressure and temperature on a shock absorber* Procedia Chemistry 1/2009 pp 88-91